Revised: 20 July 2018 | Accepted: 4 August 2018

DOI: 10.1111/jace.15997

ORIGINAL ARTICLE

Journal of the American Ceramic Society

Sintering and rounding kinetics of irregular glass particles

Raphael M. C. V. Reis[1] | **Anne J. Barbosa**[2] | **Luciana Ghussn**[3] | **Eduardo B. Ferreira**[4] | **Miguel O. Prado**[5] | **Edgar D. Zanotto**[2]

[1]Department of Metallurgical and Materials Engineering (VMT), Fluminense Federal University (UFF), Volta Redonda, Brazil

[2]Vitreous Materials Laboratory (LaMaV), Department of Materials Engineering (DEMa), Federal University of São Carlos (UFSCar), São Carlos, Brazil

[3]Department of Mechanics and Energy, Rio de Janeiro State University (UERJ), Resende, Brazil

[4]Department of Materials Engineering (SMM), São Carlos Engineering School – (EESC), University of São Paulo (USP), São Carlos, Brazil

[5]Comisión Nacional de Energía Atómica, San Carlos de Bariloche, Argentina

Correspondence
Raphael M. C. V. Reis, Department of Metallurgical and Materials Engineering (VMT), Fluminense Federal University (UFF), Volta Redonda, Brazil.
Email: raphaelmreis@gmail.com

Funding information
Brazilian National Council for Scientific and Technological Development (CNPq); National Agency for Scientific and Technological Promotion (ANPCyT), Grant/Award Number: 490634/2008-7, 143040/2008-1; São Paulo Research Foundation, Grant/Award Number: CEPID 2013/07793-6

Abstract

Compacts of irregular glass particles sinter up to five times faster than spherical-particle compacts of the same composition. This effect has been attributed to the sharp edges of irregular particles. In this article, we propose and test a phenomenological model for the sintering kinetics of jagged glass particles considering their rounding during sintering. We assume that the small radii of curvature of the particle edges increase as the particles round off and control the sintering rate. We tested the model by measuring the sintering shrinkage of spherical and irregular particle compacts of a diopside ($MgO{\cdot}CaO{\cdot}2SiO_2$) glass and using literature sintering data for particles of different shapes of a soda-lime-silica glass. The sintering rate of irregular-particle compacts is initially much higher but tends to reach that of their spherical counterparts as they round off. Our model describes the experimental shrinkage of both glasses and explains the shrinkage anisotropy of irregular-particle compacts in the initial stages of sintering, providing a significant step toward the understanding and description of the sintering kinetics of jagged glass particles.

1 | INTRODUCTION

Sintering of glass powders has been used for the fabrication of a variety of dense and porous glass and glass-ceramic products,[1,2] and may also take place in natural phenomena such as during cooling of volcanic ash.[3] Glass sintering kinetics has been modeled for a variety of conditions, usually assuming an ideal geometry.

For instance, Frenkel[4] modeled the initial stage of sintering of a pair of spherical particles by viscous flow causing the growth of a neck in the contact between them and the approach of their centers. This idea may be generalized for a simple cubic packing of identical spheres, Equation 1 after the correction of Exner and Petzow,[5] which describes the change in length of sample of spheres of radius r in a compact of initial length, L_0, at a constant temperature.

$$\frac{\Delta L}{L_0} = -\frac{3}{8}\frac{\gamma}{\eta \cdot r}t \quad (1)$$

In the case of glass particles, γ is the glass/air surface tension, η is the viscosity, and t is the sintering time at a given temperature, T. The surface tension has a weak temperature dependence, whereas the viscosity strongly varies with T. While it has been shown that Frenkel's model does not perfectly agree with experiments and finite element simulations,[6–8] his simple equation captures the physics of viscous sintering and provides a reasonable description of the initial stages of sintering of spherical glass particles.

In practice, however, glass particles prepared by traditional methods, such as crushing or milling, are far from spherical, and it is well-known that irregular particles sinter significantly faster than spherical ones.[9–11] For instance, in a classical study, Cutler and Henrichsen[9] showed that the more irregular the particles, the faster they sinter, concluding that the sharp radius of their edges at their point of contact is responsible for this effect.

The sintering kinetics of irregular particles is often described as occurring n-fold faster than their spherical counterparts,[9–12] with reported values of n between 1.8 and 5. Then, a fitting parameter is typically added to Frenkel's equation to account for their increased sintering rate.[9,10] However, experiments provide evidence[9] that the shrinkage rate of spherical-particle compacts is approximately constant during the initial stage of sintering, whereas irregular particle compacts shrink faster in the beginning, but slows down during the process. Cutler and Henrichsen[9] tentatively proposed that the nonlinearity in the shrinkage rate of irregular particle compacts is due to the "temperature equilibration and viscosity adjustment of the glass."

The driving force for sintering is the same as the driving force for the rounding of irregular particles.[13] Both phenomena take place simultaneously at high temperatures, hence jagged particles round during sintering. The rounding of vitreous particles is also technologically important for the production of glass beads, polymer pellets, and in natural phenomena, such as the rounding of vitreous ash in volcanic events.[14,15]

Interestingly, to the best of our knowledge, an analytical description of the particle shape evolution during rounding by viscous flow is still lacking, because glass particles of a variety of complex shapes exist and their analytical description is a nontrivial task. For instance, Frenkel[1] proposed an analytical model for the rounding of irregular particles by viscous flow driven by capillarity forces, considering that their surface is described by the contribution of spherical harmonics of different orders, n, weighted by a scaling parameter, q_n. The particle rounding was characterized by the decrease in q_n with time, according to Equation 2.

$$q_n = q_{0n}\exp\left(-\frac{n}{4\pi}\frac{\gamma}{\eta \cdot r}t\right) \quad (2)$$

However, it is difficult to apply this equation to the sintering of a real irregular powder.

In another example, Katsura et al[13] studied the rounding by viscous flow of a prolate ellipsoidal particle with an aspect ratio of 3 using a finite-element method. Their results show that it takes about 3-5 units of reduced time, $\tau = \gamma \cdot t/\eta \cdot r$, to reach full rounding.

In the present article, we compare the shrinkage of spherical and jagged glass particle compacts during sintering, attributing the gradual reduction in the sintering rate to particle rounding (due to the surface tension). We model the shrinkage rate of compacts of irregular particles by considering the evolution of an effective particle radius of curvature during sintering and test it for diopside and soda-lime-silica glass powders.

2 | EXPERIMENTAL PROCEDURES

2.1 | Glass and sample preparation

A diopside ($MgO{\cdot}CaO{\cdot}2SiO_2$) glass was prepared by melting crystalline diopside previously obtained by solid-state reaction among $CaCO_3$, MgO, (99.9%; JT BAKER, Phillipsburg, NJ) and fumed silica (99.8%; ALDRICH, St. Louis, MO) at 1200°C for 48 hours. We tracked the completion of the reaction by X-ray diffraction. The melting operation was performed in a platinum crucible at 1550°C for 15 minutes in a bottom-load electrical furnace. The melt was poured on a steel plate to form a disc of approximately 10 cm diameter and 1 cm thick. The glass plate was annealed at 715°C ($T_g \sim 720$°C for diopside glass[16]) for 4 hours.

The glass plate was crushed and milled in a planetary mill (PULVERISETTE–FRITSCH, Idar-Oberstein, Germany) with silicon nitride jar and balls; then the resulting powder was sieved between 38 and 75 μm nylon meshes and washed above the 38-μm mesh sieve with ethanol to remove the fine glass dust that adhered to the particles. Part of the powder was flame rounded to a spherical shape.[17] We thus considered that the jagged and resulting spherical particles have the same equivalent spherical diameter distribution, by volume.

We prepared cylindrical compacts of 3.8 mm diameter and approximately the same height for the sintering experiments using approximately 60 mg of irregular or spherical particles and anhydrous ethanol as a binder. The powders were uniaxially pressed using a small pressure of 12.5 MPa to provide a reproducible initial packing. This low pressure was chosen to avoid particle fracture. The initial relative density was determined as the ratio between

the powder mass and the volume of the mold cavity after pressing.

2.2 | Heating microscopy and scanning electron microscopy

The powder compacts were isothermally sintered in a heating microscope/optical dilatometer (MISURA HSM ODHT —EXPERT SYSTEM SOLUTIONS, Modena, Italy). The samples were heated from room temperature to the treatment temperature at 80°C/s, fast enough to minimize sintering during the heating ramp. Overshooting was minimized at 3°C maximum by carefully tuning the PID parameters in the temperature controller. The furnace was closed on both ends for increased thermal homogeneity, which was found to be ±1°C in the sample region. Optical images of the samples were digitally acquired every 5 or 10 seconds. The vertical (axial) and horizontal (radial) shrinkages were calculated by automatic determination of the sample silhouette dimensions using an ImageJ[18] macro. For the radial shrinkage, only the top half of the sample was considered to discard any possible influence of the sample holder, such as sticking and thermal lag. The sintering start ($t = 0$) was taken as the data point before the first detected reduction in sample size (ie, the maximum of the measured dilatometric expansion curve).

Compacts of spherical ("S" samples) and jagged particles ("J" samples) were sintered at 803 and 813°C, until saturation, ie, until no further shrinkage was observed. The experiments were replicated three times at 803°C and twice at 813°C. We chose these temperatures to follow the sintering kinetics in a comfortable time scale. The model fitting was done using the software Origin 8.5 (ORIGINLAB CORPORATION, Northampton, MA).

2.3 | Scanning electron microscopy

We sintered additional compacts of spherical and irregular particles for 10, 20, 40, and 60 minutes at 803°C and analyzed them by scanning electron microscopy (PHENOM—FEI, Eindhoven, the Netherlands) to evaluate particle necking and rounding during sintering.

2.4 | Glass and particle characterization

We determined the particle size distribution, PSD, of the spherical diopside glass particles by automatic image analysis of approximately 18 000 particles using an ImageJ[18] macro. We assumed that the volumetric-equivalent spherical diameter distribution of both powders is the same, since the spherical particles were prepared by spheroidizing a sample of the same irregular particles.

The glass viscosity curve, $\eta(T)$, was determined between 755 and 825°C by the indenter penetration method during continuous heating[19] in the Institute of Silicate Chemistry (St. Petersburg, Russia). With this technique, one can determine the viscosity of glasses showing prominent crystallization, with a standard error <0.1 in $\log(\eta)$. Considering the temperature to be accurate within ±2°C, due to furnace thermal gradients and thermocouple calibration, this error increases to a maximum of 0.127.

We considered a value of $\gamma = 0.343$ J/m^2 for the melt/air surface energy for diopside. This value was determined by extrapolation of existing data in the range 1400 and 1550°C.[20] The reported error for γ was only 0.01 J/m^2 (~3%), however, we considered an approximate error of 10%, to account for the extrapolation to much lower temperatures. With these three parameters, average particle radius, η and γ, we calculated $\gamma/(\eta \cdot r)$ for our diopside glass powder.

We also estimated $\gamma/(\eta \cdot r)$ by fitting the Frenkel's model to experimental data of sintering shrinkage of spherical particles. This procedure yields an effective value of this parameter for a given powder, considering the real PSD, experimental errors (eg, temperature) and any inaccuracy of Frenkel's model. Therefore, this approach is especially adequate to compare the sintering kinetics of compacts of spherical and irregular particles, since γ, η, T, and the PSD are the same for both powders.

3 | RESULTS AND DISCUSSION

3.1 | Glass characterization

Figure 1 shows the particle size distribution of the spherical particles. It is relatively narrow, with approximately 90% of the particles between 50 and 100 μm. Considering a normal distribution, we have an average particle size of 76 μm with a standard deviation of 17 μm (22%). The distribution of Figure 1 also represents the volumetric-

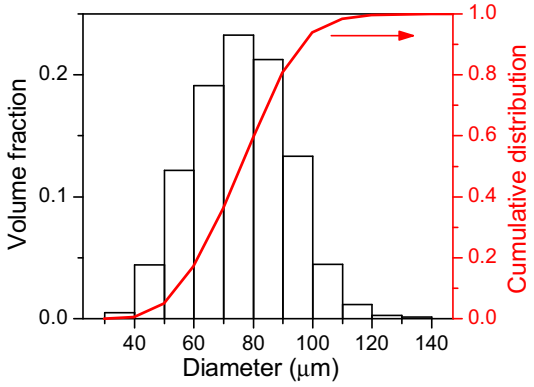

FIGURE 1 Particle size distribution of the spherical diopside glass particles

equivalent diameter of the irregular particles, since the spherical particles were produced from a sample of the same irregular particles.

The viscosity curve of our diopside glass between 755°C and 825°C is shown in Figure 2. The Vogel-Fulcher-Tamman expression (VFT) was fit to the data, resulting in $\log(\eta/\mathrm{Pa}\cdot\mathrm{s}) = -5.089 + 4253.0\,\mathrm{K}/(T - 752.9\,\mathrm{K})$, yielding 1.2×10^8 and 4.8×10^7 Pa·s, at 803 and 813°C, respectively.

Table 1 shows the values of $\gamma/(\eta{\cdot}r_0)$ calculated using measured parameters and obtained by fitting Frenkel's model to the initial shrinkage of the spherical particles, which behaves linearly between 2% and 9% shrinkage (Figure 3).

The calculated $\gamma/(\eta \cdot r_0)$ are approximately three times higher than the fitted values. However, the uncertainty in the calculated values is much higher than in the fitted ones. The fitted $\gamma/(\eta \cdot r_0)$ avoids measurement errors of the powder properties, but are affected by the intrinsic imperfection in Frenkel's model. To test our model (Section 3.3), we chose to use the fitted values of $\gamma/(\eta{\cdot}r_0)$ since they best describe the sintering of the spherical particles. In this way, we can isolate the influence of the particle irregularity in the sintering kinetics. However, it should be stressed that this procedure demands previous sintering experiments with spherical particles.

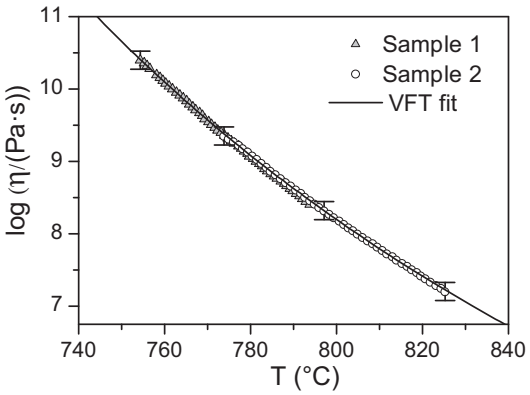

FIGURE 2 Viscosity of the diopside glass used in this study

TABLE 1 Viscous sintering parameters calculated from the glass properties and by fitting Frenkel's model to the sintering data of spherical-particle compacts

Powder	Sintering temperature (°C)	$\gamma/\eta{\cdot}r_0$ (s^{-1}) Calculated from glass properties	$\gamma/\eta{\cdot}r_0$ (s^{-1}) Fit parameter in Frenkel's model
Spherical diopside (38-75 μm)	803	8 (4) × 10^{-5}	3.305 (4) × 10^{-5}
	813	19 (9) × 10^{-5}	6.34 (2) × 10^{-5}

The values in parentheses indicate the last-digit standard error.

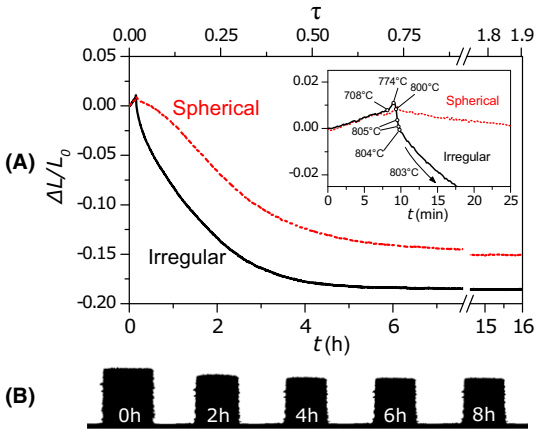

FIGURE 3 Results of a heating microscopy experiment. A, Shrinkage of samples S1 and J1. The inset shows the initial stages of sintering. B, Images of sample J1 at different sintering times

3.2 | Linear shrinkage and particle rounding

Figure 3A shows the radial shrinkage of two typical samples of spherical (S1) and irregular (J1) particles during sintering. Figure 3B shows pictures of the sample J1 silhouette at five distinct moments. The heating ramp took about 9 minutes and was followed by an isothermal dwell of 16 hours at 803°C. Sample J1 sintered faster than S1, which reached the saturation density after approximately 8 and 13 hours of heat treatment, respectively.

The inset of Figure 3A shows the first minutes of the analysis. During heating, an abrupt change in thermal expansion coefficient at T_g(~720°C) takes place at 8 minutes. At the same time, there is a small drop in the curve for the compact of spherical particles caused by the glass relaxation towards the supercooled liquid curve. This relaxation process is more evident for the spherical particles since, after production by the flame rounding process, they were cooled at a much higher rate than the parent glass. Hence, they have a higher fictive temperature, which is also inferred from the different relaxation behaviors at T_g in the differential scanning calorimetry traces of the two powders (not shown).

Sample J1 shows a larger total shrinkage, which can be accounted for by two main factors: (a) the initial relative density for irregular-particle compacts (0.48) was lower than that for spherical ones (0.52), hence the irregular-particle compact may shrink more until saturation densification; (b) surface crystallization prevents full densification of the particle compacts and, since the spherical particles initially sinter at a lower rate, surface crystallization may stop densification at a lower level. In the initial stage of sintering, which is the focus of this paper, crystallization was

negligible, since no crystals were observed on the particles surfaces.

The shrinkage of compact S1 (spherical particles) seems to be reasonably linear with time for the first 10% shrinkage, for which Frenkel's model should be valid. On closer inspection, however, the shrinkage rate for the first 1% shrinkage is approximately half the rate of the next 8% shrinkage.

Sample J1 (jagged particles) behaves much less linearly: initially, it sinters much faster than S1, but slows down with time, reaching about the same shrinkage rate (curve slope) of S1 at around 90 minutes (12% shrinkage). Hence, the sintering rate of irregular particles changes drastically in the initial minutes of sintering. In the first 40 seconds, the irregular-particle compact shrinks about 500 times faster than its spherical counterpart does. Then, in the next minutes, it shrinks about 50 times faster than the spherical one. This strong variation is likely caused by the very sharp edges of the irregular particles, which, in contact with neighbor particles lead to very fast sintering, or by the rearrangement of the irregular particles due to the lower initial packing density. This effect is observed for all samples of jagged particles, but not for the spherical particles. Temperature overshooting is not the cause of this behavior since it was similar for both types of compacts.

Rounding can explain the drop in the shrinkage rate of the irregular particles. Figure 4 shows spherical and irregular particles sintered for different times at 803°C. Particle rounding is seen during the first 60 minutes of sintering. The spherical particles show little shape change and necking, which corroborates the sintering curve of Figure 3. The circles in the micrographs of the jagged particles in Figure 4 represent the effective sintering diameter at each time, calculated with our model (presented in Section 3.4).

3.2.1 | Shrinkage anisotropy

Figure 5 shows the axial (vertical) and radial (horizontal) shrinkages of the spherical- and irregular-particle compacts at 803°C. Their shrinkage is markedly anisotropic. For the spherical particles, the shrinkage is initially equal in both directions, but becomes anisotropic towards the end, after about 2-3 hours of sintering, with a greater axial shrinkage. This effect may result from anisotropic particle packing, particle rearrangement[21] or gravitational effects.[22]

For the irregular particles, however, the opposite behavior was observed—the shrinkage is initially faster in the radial direction, which was also observed by other authors.[11,23,24] This behavior may arise from packing anisotropy, as suggested by Giess et al.[23] Irregular particles tend to align horizontally on their largest face in the compact, and thus with their sharpest corners radially aligned, increasing the shrinkage rate in this direction.

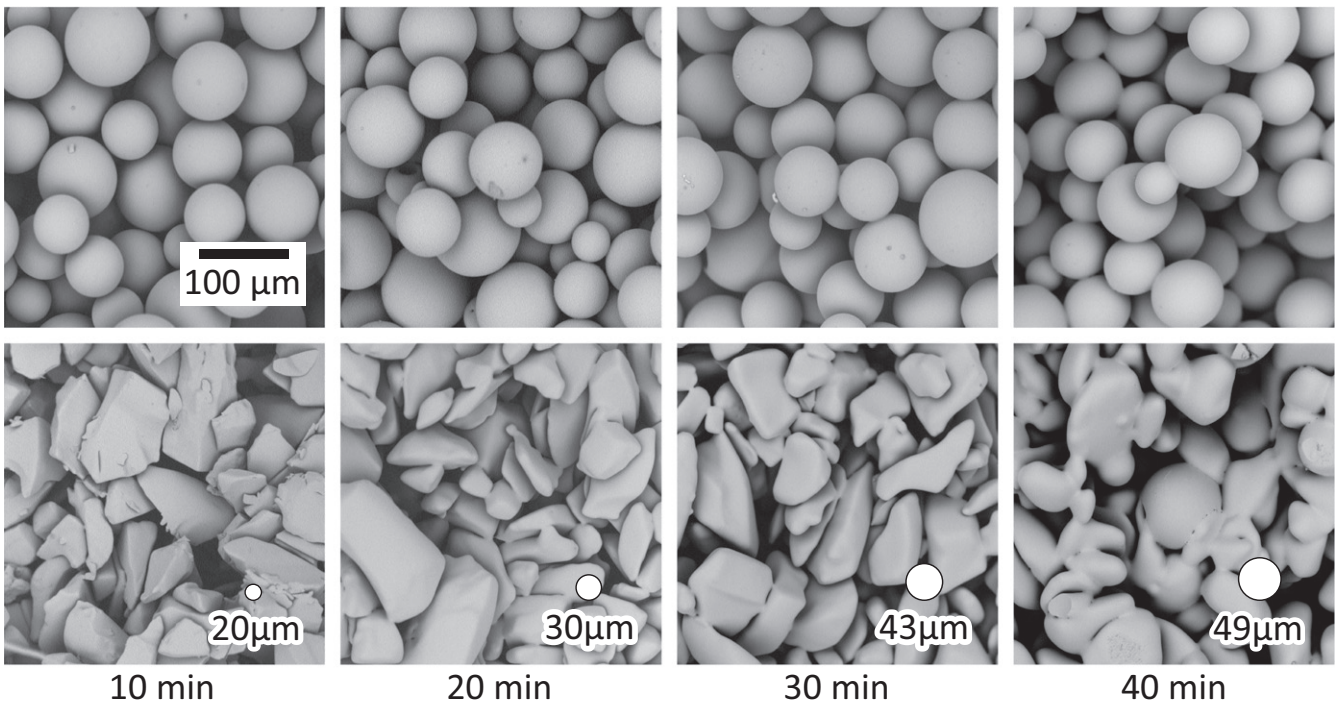

FIGURE 4 SEM micrographs of spherical (top) and irregular particles (bottom) sintered at 803°C for different time intervals, showing rounding of the irregular particles during sintering. The small circles represent the effective diameter of curvature calculated by the proposed model at each sintering time

For the irregular particle compacts, after 2-3 hours of sintering, the radial shrinkage also slows down faster than the axial shrinkage, which indicates that the same phenomena that lead to the shrinkage anisotropy of the spherical-particle compacts also take place for the jagged ones.

The final shrinkage of a compact of jagged particles can be isotropic due to the fortuitous combination of two opposing effects: the faster radial shrinkage at the initial stages of sintering due to the horizontal alignment of particles smallest radius of curvature, and the greater axial shrinkage at the final stages due to the anisotropic particle packing, or gravity effect (as observed for the spherical particles).

The sintering anisotropy of elongated particle compacts is a complex subject. Cannon and Raj[25] demonstrated that enhanced shrinkage may change from the radial to the axial direction during sintering, whereas Tikare and Braginsky[26] showed that, depending on particle packing, the shrinkage may be greater in either direction.

3.3 | Model: sintering and rounding of irregular particles

We assumed that the radius of curvature of the particle edges controls the sintering rate of jagged glass powder compacts. These local radii round off during sintering increasing their size up to the particle's equivalent (by volume) spherical radius. This fact can explain the gradual reduction in the sintering rate of irregular particles. Therefore, one could change the Frenkel model to account for this effect assuming that the sintering rate of a powder compact depends on the edge radius of curvature, $h(t)$, rather than the particle's equivalent spherical radius, r, Equation 3.

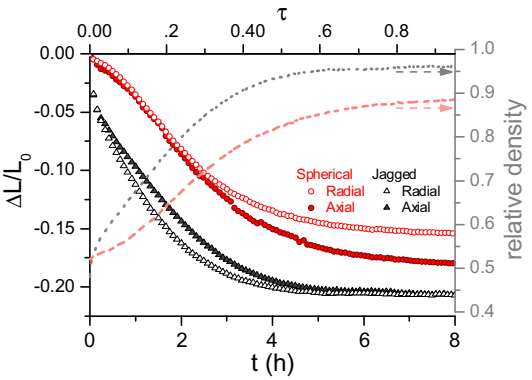

FIGURE 5 Linear shrinkage and densification of spherical and jagged diopside powders sintered at 803°C

$$\frac{d(\Delta L(t)/L_0)}{dt} = -\frac{3}{8}\frac{\gamma}{\eta \cdot h(t)} \tag{3}$$

We have chosen the Frenkel model to analyze the effect of particle shape on sintering due to its simple mathematical form and reasonable applicability. We avoided the model's inaccuracies by "calibrating" it to the shrinkage of the spherical-particle compacts, as explained in Section 3.1.

The edge radius of curvature depends on the particle irregularities, such as sharp edges and the smallest thickness of particles with high aspect ratio. We propose that $h(t)$ starts as a small value, h_0, and increases as the particle rounds up to a maximum that equals the particles' equivalent spherical radius, r_0. Also, the rounding rate is proportional to: (a) the relative difference between the edge radius and the particle's equivalent spherical radius, assuring that the rounding rate diminishes with time and tends to zero as $h(t) \to r_0$; (b) γ/η, which controls viscous flow and; (c) an empirical constant B.

Thus, the rounding rate is given by:

$$\frac{dh(t)}{dt} = B\frac{\gamma}{\eta}\left(\frac{r_0 - h(t)}{r_0}\right) \tag{4}$$

Solving Equation 4 for $h(t)$ and applying the boundary condition $h(0) = h_0$, we get:

$$h(t) = r_0\left(1 - \left(1 - \frac{h_0}{r_0}\right) \cdot \exp\left(-B\frac{\gamma}{\eta \cdot r_0}t\right)\right) \tag{5}$$

Combining Equations 3 and 5 and integrating, we get:

$$\frac{\Delta L(\tau)}{L_0} = -\frac{3}{8}\left(\tau + \frac{\ln(1-(1-A)\exp(-B\cdot\tau)) - \ln(A)}{B}\right) \tag{6}$$

where $A = h_0/r_0$ and $\tau = \gamma t/\eta r_0$ is the reduced time. The first term in the right-hand side of Equation 6 is simply the Frenkel equation of sintering. The second term represents the additional shrinkage due to the sharp radius of curvature of the jagged particles. For $t = 0$ the total shrinkage is zero, whereas for sufficiently long times the second term becomes $-\ln(A)/B$, which is the excess shrinkage compared with the spherical particles due to the jagged particle irregularities, at the end of the initial sintering stage. The model works as expected: the sharper the radius (smaller A) the faster the shrinkage. In addition, the larger the value of B, the faster the rounding and, thus, the smaller the excess shrinkage due to irregularities.

In the proposed model for irregular particles, as they round off, the difference between the particle radius and the edge radius falls exponentially with $B{\cdot}\tau$, Equation 5. The term $\gamma t/\eta r$ $(= \tau)$ also appears in the exponential

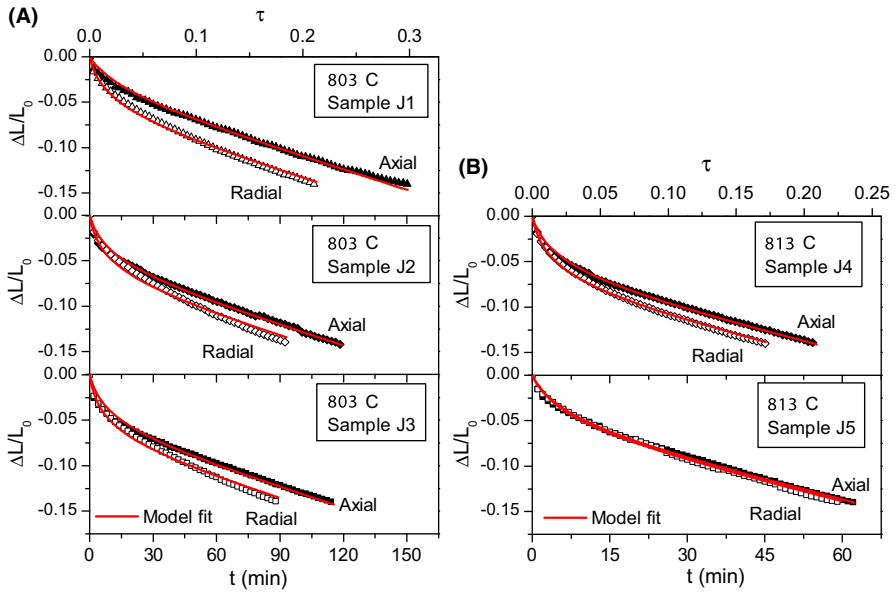

FIGURE 6 Experimental and calculated shrinkage of irregular diopside powders sintered at (A) 803°C and (B) 813°C

TABLE 2 Fitting parameters from the sintering kinetics of diopside glass compacts of irregular particles

Sintering temperature (°C)	Sample	Direction	$A = h_0/r_0$	B
803	J1	Axial	0.210 (2)	16.7 (1)
		Radial	0.073 (1)	16.7 (1)
	J2	Axial	0.089 (1)	16.7 (1)
		Radial	0.052 (1)	16.7 (1)
	J3	Axial	0.078 (1)	16.7 (1)
		Radial	0.045 (1)	16.7 (1)
813	J4	Axial	0.078 (1)	15.3 (1)
		Radial	0.046 (1)	15.3 (1)
	J5	Axial	0.122 (1)	15.3 (1)
		Radial	0.111 (1)	15.3 (1)

The values in parentheses indicate the last-digit standard error.

decrease in the spherical harmonics contribution in Frenkel's rounding model, Equation 2.

3.4 | Fitting

We fit Equation 6 to the shrinkage data of the irregular diopside glass powder using A and B as free parameters. The fitting results are shown in Figure 6 and Table 2. The values in parentheses in Table 2 indicate the last-digit standard error. For a given temperature, all curves (including both axial and radial shrinkage) were fit simultaneously constraining the fitting to a common B (which is an empirical constant). The constraint in B was imposed to allow the comparison of A between samples sintered at each temperature.

The fitted values for A (Table 2) in the radial direction are lower than the axial one, indicating a smaller curvature radius contributing to sintering in this direction, which is consistent with the irregular particles having their sharpest corners radially aligned.

We calculated the instantaneous radius of curvature, $h(t)$, using Equation 5 with $A = 0.1$ and $B = 16.7$ for the sintering times of the Figure 4 micrographs. The circles drawn on each micrograph represent the calculated diameters, which are consistent with the rounding of the irregular particles sharp edges. The sintering rates of the spherical and irregular particles calculated using these same values of A and B are shown in the Graphical Abstract (Figure S1).

We also tested our model using the experimental data of Cutler and Henrichsen[9] for compacts of soda-lime-silica glass particles of granulometry between 170 and 140 mesh (approximately 90 and 105 μm), with different roundness and sintered at 672°C for different times. Particles of different roundness were prepared by: (a) partially sintering at ~670°C and crushing the compact; (b) passing the particles through a furnace at 1100°C (partial rounding) and (c) passing the particles through a furnace at 1200°C (full rounding).[9] We found $\gamma/(\eta \cdot r_0) = 2.68(3) \times 10^{-5}\ s^{-1}$ by fitting Frenkel's model to the linear portion of the shrinkage curve of the spherical particles at 672°C. The results are shown in Figure 7 and Table 3.

Our model accurately describes the shrinkage of these irregular particles, with values of A between 0.04 and 0.21, which reasonably indicate an initial effective radius of curvature of 4%-21% of the particle radius (1.0 means perfect sphere). The more spherical the particles, the larger the value of A, indicating a larger initial radius of curvature due to particle roundness.

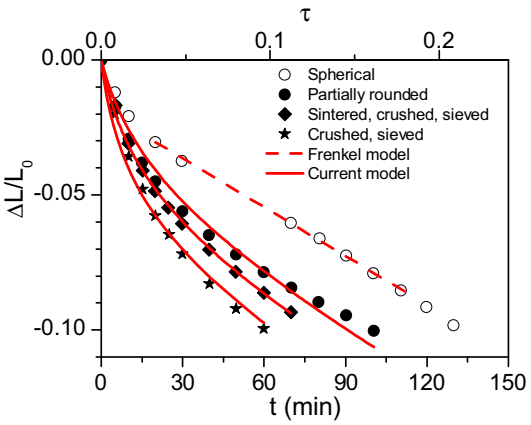

FIGURE 7 Linear shrinkage of compacts of soda-lime-silica glass particles of different shapes at 672°C. Our model fits are shown by full lines and the experimental data of Cutler and Henrichsen[9] are shown by symbols

TABLE 3 Fitting parameters from the sintering kinetics of particles of a soda-lime-silica glass of different irregularity levels[9]

Powder	Direction	$A = h_0/r_0$	B
Partially rounded	Axial	0.15 (1)	14.7 (9)
Sintered, crushed, sieved	Axial	0.11 (1)	14.7 (9)
Crushed, sieved	Axial	0.07 (1)	14.7 (9)

The values in parentheses indicate the last-digit standard error.

The values of B for the jagged diopside and soda-lime-silica glass particles sintered at different temperatures are very close, averaging $B = 16$. If B is set free to best fit each curve, it varies between 11 and 28, and then even better fittings are obtained. This relatively narrow range suggests that B could possibly be taken as a constant, with a typical value of 16. This assumption allows the application of the model using only one fitting parameter, A, which substantially improves its applicability to jagged particles of different glasses.

Our model accurately describes the experimental shrinkage data, even though it simplifies details of the particle's irregularities, such as different shapes and the distribution of edge curvature radius into a single value, h_0.

3.5 | Final considerations

We considered the effect of irregular particle fine edges on sintering and modeled their decreasing influence as they round off during sintering. However, the interaction between rounding and sintering (and implicitly sintering anisotropy) is a much more complex and still unresolved problem, as exemplified by the works of Cannon and Raj[25] and Tikare and Braginsky.[26] Particle rounding changes the effective sintering radius, which is the main focus of this work. However, rounding also changes the particle characteristic lengths, which results in size changes (eg, the largest dimension of a particle shrinks, while the smallest increases). We did not consider this complexity in our model.

Sintering may also have an effect on rounding. As the particles sinter, in the final stage their edges and surfaces are eliminated and full particle rounding may not be observed during sintering of a jagged-powder compact. This can be inferred by comparing the typical reduced times for full sintering of a powder compact ($\tau < 1$),[7,24,this work] the rounding of a spheroid particle ($\tau \sim 3$-5),[13] and the sintering and rounding of two spherical particles ($\tau \sim 10$).[27] Our results show that the initial particle shape does not significantly influences the final stages of sintering after $\tau \sim 0.2$, when individual particles no longer exist.

A comparison of the rounding kinetics observed in this work and the simulations of Katsura et al[13] for spheroid particles provides interesting insights. However, we emphasize that Katsura's particles are smooth ellipsoids of revolution, while our ground particles have irregularities in different scales. We may simplify such irregularities to two scales: the particle aspect ratio and the fine jagged edges. In their simulation, full rounding of a spheroid particle with an aspect ratio $c/a = 3$ took about 3-5 units of reduced time, $\tau = \gamma t/\eta r$, which is much longer than our sintering experiments. However, their results qualitatively agree with our experimental data: Figure 4 shows that after 60 minutes ($\tau = 0.12$) the particles retain an aspect ratio >1, even though the sharp edges are mostly rounded.

We have shown that after 90 minutes ($\tau = 0.18$) the jagged and spherical particles begin to shrink at approximately the same rate. This means that the effect of particle irregularities on shrinkage is restricted to the initial stage of sintering. This correlates with two phenomena: (i) the rounding of the fine particle edges, as shown in Figure 4, and (ii) a change in sintering mechanism from neck-growth to pore-shrinkage (after that, the initial particle shape is not as significant).

This raises two non-excluding hypotheses: (a) The correlation with fine edge rounding (phenomenon i) may indicate that it is the particle's fine edges (their "jaggedness") that contributes the most to the enhanced shrinkage of irregular particle compacts, and not their higher aspect ratio. As the fine radius round or sinter to other particles, the sintering rate tends to that of spherical particles. (b) The change in sintering mechanism (ii) may imply that the parameter B is fit to a value that forces the sintering rate of both samples to become the same, not because of the rounding kinetics, but because of sintering kinetics. In this sense, $B = 16$ may overestimate the rounding kinetics of a typical particle. The rather

similar values of B obtained for different powders and temperatures are consistent with this hypothesis since, assuming negligible crystallization and similar particle shapes, the sintering curves of different glass powders become similar when plotted against reduced time.[24] Further experiments and simulations are needed to assess which of these hypotheses actually play a significant role in the slowing down of the shrinkage kinetics. In both cases, the particle shape should not influence sintering significantly after $\tau \sim 0.2$.

4 | CONCLUSIONS

The sintering kinetics of compacts of irregular glass particles are initially much faster than those of their spherical counterparts due to the sharper radii of curvature of the jagged particle edges. However, during sintering, these sharp edges round off, gradually increasing in radius and approaching the particle's equivalent spherical diameter, therefore, the shrinkage rate continuously diminishes, tending to that of the spherical particles. Our results also indicate that after the initial sintering stage, the shrinkage rate is no longer significantly influenced by the initial shape of the particles.

The marked sintering anisotropy of the irregular-particle compacts in the initial stages is readily explained by the preferential orientation of the particles with their sharper edges radially aligned (smaller radii of curvature), leading to a faster shrinkage in that direction. On the other hand, compacts of spherical particles initially sintered isotropically, however, in the final stages, their vertical shrinkage became greater than the radial shrinkage, which we attribute mostly to gravitational effects. Surprisingly, however, for the jagged particle compacts, the fortuitous combination of much faster radial shrinkage during the initial stages and greater vertical shrinkage at the final stages resulted in isotropic shrinkage.

Overall, our model captured well the effect of particle rounding on sintering using only one fitting parameter, $A = h_0/r_0$, which is the ratio between the initial radius of curvature of the irregular particle edges and the effective spherical particle radius. Therefore, this new phenomenological model provides a significant step towards understanding and describing the sintering kinetics of irregular glass particle compacts.

ACKNOWLEDGMENTS

This work was supported by the Brazilian National Council for Scientific and Technological Development (CNPq), the National Agency for Scientific and Technological Promotion (ANPCyT) [grant numbers 490634/2008-7 and 143040/2008-1], and by the São Paulo Research Foundation (FAPESP) CeRTEV Project [CEPID 2013/07793-6]. We also thank the two anonymous reviewers for their insightful comments, which significantly improved this paper.

ORCID

Raphael M. C. V. Reis http://orcid.org/0000-0002-0540-1511

REFERENCES

1. Müller R, Reinsch S. Viscous-phase silicate processing. In: Bansal N, Boccaccini AR, editors. *Ceramics and composites processing methods*. Hoboken, NJ: John Wiley & Sons, 2012; p. 75–144.
2. Soares VO, Peitl O, Zanotto ED. New sintered Li_2O–Al_2O_3–SiO_2 ultra-low expansion glass-ceramic. J Am Ceram Soc. 2013;96(4):1143–49.
3. Wadsworth FB, Vasseur J, von Aulock FW, Hess KU, Scheu B, Lavallée Y, et al. Nonisothermal viscous sintering of volcanic ash. J Geophys Res Solid Earth. 2014;119:8792–804.
4. Frenkel J. Viscous flow of crystalline bodies under the action of surface tension. J Phys (USSR). 1945;9(5):385–91.
5. Exner HE, Petzow G. Shrinkage and rearrangement during sintering of glass spheres. Paper presented at: 4th International Conference on Sintering and Related Phenomena 1975. In: Kuczynski GC, editor. *Sintering and catalysis*. Notre Dame, IN; New York, NY: Plenum Press, 1975; p. 279–93.
6. Martínez-Herrera JI, Derby JJ. Viscous sintering of spherical particles via finite element analysis. J Am Ceram Soc. 1995;78(3):645–9.
7. Jagota A, Dawson PR. Micromechanical modeling of powder compacts—I. Unit problems for sintering and traction induced deformation. Acta Metall. 1988;36(9):2551–61.
8. Wakai F, Katsura K, Kanchika S, Shinoda Y, Akatsu T, Shinagawa K. Sintering force behind the viscous sintering of two particles. Acta Mater. 2016;109:292–9.
9. Cutler IB, Henrichsen RE. Effect of particle shape on kinetics of sintering of glass. J Am Ceram Soc. 1968;51(10):604–5.
10. Prado MO, Fredericci C, Zanotto ED. Glass sintering with concurrent crystallization: part 2. Nonisothermal sintering of jagged polydispersed particles. Phys Chem Glasses. 2002;43(5):215–23.
11. Müller R, Eberstein M, Reinsch S, Schiller WA, Deubener J, Thiel A. Effect of rigid inclusions on sintering of low temperature co-fired ceramics. Phys Chem Glass Eur J Glass Sci Technol B. 2007;48(4):259–66.
12. Soares VO, Reis RMCV, Zanotto ED, Pascual MJ, Durán A. Non-isothermal sintering with concurrent crystallization of polydisperse jagged Li_2O-Al_2O3-SiO_2 glass particles: simulation and experimental results. J Non-Cryst Solids. 2012;358:3234–42.
13. Katsura K, Shinoda Y, Akatsu T, Wakai F. Sintering force behind shape evolution by viscous flow. J Eur Ceram Soc. 2015;35:1119–22.
14. Sachs M, Schmidt J, Toni F, Blümel C, Winzer B, Peukert W, et al. Rounding of irregular polymer particles in a downer reactor. Procedia Eng. 2015;102:542–9.
15. Wadsworth FB, Vasseur J, Llewellin EW, Genareau K, Cimarelli C, Dingwell DB. Size limits for rounding of volcanic ash particles heated by lightning. J Geophys Res Solid Earth. 2017;122:1977–89.

16. Reis RMCV, Fokin VM, Zanotto ED. Determination of crystal growth rates in glasses over a temperature range using a single DSC run. J Am Ceram Soc. 2016;99(6):2001–8.
17. Watkinsa IG, Prado M. Mechanical properties of glass microspheres. Procedia Mater Sci. 2015;8:1057–65.
18. Rasband WS. *ImageJ*. Bethesda, MD: U.S. National Institutes of Health, 1997–2012. Available from http://imagej.nih.gov/ij/. Accessed August 21, 2018.
19. Klyuev VP. Indenter-penetration viscometry of glasses for small-sized samples under conditions of continuous heating. Glass Phys Chem. 2000;26(6):559–65.
20. Taniguchi H. Surface tension of melts in the system $CaMgSi2O_6$-$CaAI_2Si_2O_8$ and its structural significance. Contrib Mineral Petrol. 1988;100:484–9.
21. Wakai F, Chihara K, Yoshida M. Anisotropic shrinkage induced by particle rearrangement in sintering. Acta Mater. 2007;55:4553–66.
22. Olevskyy EA, German RM. Effect of gravity on dimensional change during sintering – I. Shrinkage anisotropy. Acta Mater. 2000;48:1153–66.
23. Giess EA, Fletcher JP, Herron LW. Isothermal sintering of cordierite-type glass powders. J Am Ceram Soc. 1984;67(8):549–52.
24. Prado MO, Zanotto ED, Müller R. Model for sintering polydispersed glass particles. J Non-Cryst Solids. 2001;279:169–78.
25. Cannon WR, Raj PM. Evolution of sintering anisotropy using a 2D finite difference method. J Am Ceram Soc. 2009;92(7):1391–5.
26. Tikarew V, Braginsky M. Numerical simulation of anisotropic shrinkage in a 2D compact of elongated particles. J Am Ceram Soc. 2005;88(1):59–65.
27. Pokluda O, Bellehumeur CT, Machopoulos J. Modification of Frenkel's model for sintering. AIChE J. 1997;43(12):3253–6.

SUPPORTING INFORMATION

Additional supporting information may be found online in the Supporting Information section at the end of the article.

How to cite this article: Reis RMCV, Barbosa AJ, Ghussn L, Ferreira EB, Prado MO, Zanotto ED. Sintering and rounding kinetics of irregular glass particles. *J Am Ceram Soc*. 2018;00:1–10. https://doi.org/10.1111/jace.15997